Clays and Clay Minerals, Vol. 47, No. 4, 458–465, 1999.

PARTIAL STABILIZATION OF Fe(II) IN REDUCED FERRUGINOUS SMECTITE BY Li FIXATION

PETER KOMADEL,[1] JANA MADEJOVÁ,[1] AND JOSEPH W. STUCKI[2]

[1] Institute of Inorganic Chemistry, Slovak Academy of Sciences, SK-842 36 Bratislava, Slovakia
[2] Department of Natural Resources and Environmental Sciences, University of Illinois, Urbana, Illinois 61801, USA

Abstract—Partial stabilization of Fe(II) in chemically reduced smectite, which normally readily undergoes reoxidation in air, was achieved. The purpose of this study was to determine if Fe(II) can be stabilized in reduced smectites by Li fixation upon heating. More than 80% of total Fe in ferruginous smectite SWa-1 was reduced to Fe(II) using the citrate-bicarbonate-dithionite (CBD) method while purging the clay dispersion with N_2. The reduced smectite was Li-saturated, washed free of excess ions, freeze-dried, and heated in N_2 atmosphere at 260°C for 24 h to produce Li-fixation. This treatment caused partial stabilization of Fe(II) in the clay structure. Chemical analysis, Mössbauer spectroscopy, and Fourier transform infrared (FTIR) spectroscopy proved that >20% of total Fe was Fe(II) after reoxidation with oxygen in a water dispersion, a treatment which causes complete reoxidation of Fe(II) in reduced Na-smectites. Decomposition of the OH-stretching band evident in the IR spectra indicated migration of Li into the vacant octahedra. Some of the OH groups in the reoxidized smectite were found in local trioctahedral configurations, associated with the AlFe(II)Li or Fe(III)Fe(II)Li groupings of central atoms in the octahedral sheet.

Key Words—Ferric, Ferrous, Ferruginous Smectite, Infrared Spectroscopy, Li Fixation, Mössbauer Spectroscopy, Oxidation, Reduction, SWa-1.

INTRODUCTION

Reduction of structural Fe in 2:1 dioctahedral smectites profoundly affects many fundamental properties of the clay, including layer charge, cation exchange capacity, cation fixation, swelling pressure and water-holding capacity, specific surface area, hydraulic conductivity, color, and magnetic exchange interactions (Stucki, 1988; Shen *et al.*, 1992). Because clays are ubiquitous in nature and used extensively in industry, but their natural properties are sometimes less than optimum for a particular purpose, the ability to manipulate the oxidation state to modify clay properties *in situ* can be of great benefit to agriculture, industry, and the environment. For example, the ideal site for a land-fill project would be one where the swelling and permeability of underlying soils and sediments is minimal, but sometimes other factors preclude such sites. In this case, the ability to modify these properties *in situ*, even temporarily, could overcome various adverse consequences associated with these limitations. In many situations, however, such benefits to agriculture or industry depend on the stability of the reduced oxidation state. Previous work indicates that if the smectite is Na saturated, reoxidation in water is rapid and complete, if oxygen is present (Komadel *et al.*, 1990, 1995). In the presence of K, however, reoxidation is less complete and becomes even less so with multiple redox cycles (Shen and Stucki, 1994), presumably due to the collapse of adjacent 2:1 layers around the K^+ ion.

Another method for modifying the properties of dioctahedral smectites is to heat the clay in the presence of Li^+, causing the small Li^+ ions to enter the 2:1 layer structure, which decreases the layer charge, expandability, and cation exchange capacity (Hofmann and Klemen, 1950). Upon heating, the Li^+ is attracted to negatively charged octahedral sheets. This phenomenon, along with the accompanying irreversible collapse of the layers, was proposed to be the criterion to distinguish montmorillonite from clays which have no octahedral charge, such as beidellite and nontronite (Greene-Kelly, 1953; Lim and Jackson, 1986). In smectites with tetrahedral charge, however, Li^+ can be trapped in the hexagonal cavities of the tetrahedral sheet (Calvet and Prost, 1971; Alvero *et al.*, Madejová *et al.*, 1996; Theng *et al.*, 1997). A series of reduced-charge clays was prepared from various starting Li^+-saturated montmorillonites by heating them for 24 h at 105–220°C. Higher reduction of the layer charge, increasing content of pyrophyllite-like layers, decreasing swelling and sorption ability, and slower dissolution in HCl with increasing preparation temperature were reported (Calvet and Prost 1971; Bujdák *et al.*, 1991, 1992a, 1992b, 1993; Bujdák and Slosiariková, 1994; Madejová *et al.*, 1996; Komadel *et al.*, 1996a).

Isomorphous substitution is the common means by which an octahedral sheet becomes negatively charged, but increased charge also occurs upon the reduction of structural Fe(III) to Fe(II), which may also lead to increased fixation of Li upon heating. In this case, Li substitution could assist in the stabilization of structural Fe(II) by decreasing the charge deficit in the octahedral sheet and thereby diminishing the extent to which Fe(II) reoxidation can occur. Indeed,

under these conditions, Fe(II) reoxidation would reverse the charge if no ancillary compensatory processes were involved. The purpose of the present study was to test this possibility.

MATERIALS AND METHODS

Materials

The clay used in this study was ferruginous smectite sample SWa-1 (Grant County, Washington, USA), obtained from the Source Clays Repository of the Clay Minerals Society, Columbia, Missouri, USA. The clay mineral was fractionated to <2 μm, Na^+-saturated (Na-SWa), washed free of excess salts, and freeze-dried prior to use in the experiments. The structural formula as calculated from X-ray fluorescence (XRF) data (Breen *et al.*, 1997) for the fine fraction used in this study is $M^+_{0.88}(Si_{7.32}\ Al_{0.68})(Al_{0.92}\ Fe_{2.83}\ Mg_{0.27})O_{20}(OH)_4$.

Iron reduction and Li-fixation

Iron in the clay mineral was reduced using the citrate-bicarbonate-dithionite (CBD) method while purging the clay suspension with N_2 (Komadel *et al.*, 1990). The exchangeable Na^+ in the reduced smectite (NaS-r) was exchanged by Li^+(LiS-r) and washed free of excess salts using a controlled-atmosphere liquid exchanger (updated, commercially-available version of that described by Stucki *et al.*, 1984) to minimize reoxidation, freeze-dried, and analyzed for Fe(II) and total Fe using the 1,10-phenanthroline method of Komadel and Stucki (1988). This clay mineral was packed into Al foil and placed in a quartz tube which was purged with N_2 and preheated to 260°C. The tube was kept in a tube furnance at this temperature for 24 h to invoke Li fixation. After heating, the sample (LiS-rh) was divided into two parts: one was analyzed for Fe(II) and total Fe; and the other (LiS-rho) was resuspended in H_2O and reoxidized for 2 h by bubbling O_2 (Komadel *et al.*, 1990), washed free of excess salts, freeze-dried, and analyzed for Fe(II) and total Fe by both the 1,10-phenanthroline method and Mössbauer spectroscopy. To compare the effect of Fe(III) reduction in SWa-1 on Li-fixation, Li-saturated unreduced SWa-1 was heated similarly to LiS-rh, *i.e.*, for 24 h at 260°C (LiS-h). Effects of the various treatments on the clay mineral structure were monitored by Fourier transform infrared (FTIR) spectroscopy.

Mössbauer spectroscopy

Mössbauer spectra were obtained at 100 K using a Ranger Scientific MS-900 spectrometer equipped with a ^{57}Co in 10% Rh source and a Technology Systems cryostat, then analyzed with a *least-squares* computer program assuming Lorentzian-line shapes. The areas and widths of the two members of each doublet were constrained to be equal.

FTIR spectroscopy

Infrared spectra were obtained using the KBr pressed-disk technique and a Nicolet Magna 750 FTIR spectrometer equipped with a DTGS detector. For each sample, 128 scans were recorded in the 4000 to 400 cm^{-1} spectral range in the absorbance mode with a resolution of 4 cm^{-1}. The Na-saturated samples were analyzed as thin films with a MIDAC 2000 FTIR spectrometer with a DTGS detector. In this case, 50 scans were recorded with a resolution of 1 cm^{-1}. Decomposition of the OH-stretching band into components was employed using a *least-squares* peak fitting program with the Gauss-Lorentz form of each band component and linear baseline. The convergence criterion was six significant digits for χ^2, and goodness-of-fit was evaluated at the 95% confidence interval. The assignment of individual OH components to certain pairs of octahedral atoms for untreated SWa-1 is based on the crystallochemical formula as calculated from the XRF analysis (Breen *et al.*, 1997), and on the peaks found in the OH-bending region. A minimal number of component bands was used in the fitting procedure, therefore only one component for each of the groupings Fe(III)Fe(III) and AlAl was included in the band analysis, which is less than in the previously published decomposition of SWa-1 (Madejová *et al.*, 1994). Based on chemical analysis, a small amount of Mg (0.27 per $O_{20}(OH)_4$) is present in the octahedral sheet, and therefore AlMg pairs were not included in the deconvolution, as only a negligible contribution of this band to the complex OH band is expected. To check the correctness of the decomposition (number and assignment of the OH components), the Fe content calculated from the FTIR spectrum according to Slonimskaya *et al.*, (1986) was compared with that obtained from the chemical analysis (CA). The coefficients obtained for Fe in the structural formula ($C_{IR}(Fe) = 2.85$ and $C_{CA}(Fe) = 2.83$) confirmed reasonable fitting of the OH band. Inclusion of the broad absorption band near 3400 cm^{-1} for adsorbed water as one or two components in the fitting procedure was reported to be an effective way of correcting for background due to water absorption (Slonimskaya *et al.*, 1986; Madejová *et al.*, 1994; Besson and Drits, 1997a).

RESULTS AND DISCUSSION

Chemical analysis and Mössbauer spectroscopy

Upon chemical reduction of structural Fe(III), the color of Na-SWa-1 suspensions changes from yellow through green, blue-green, dark blue and light blue to light gray. Over 80% of the total Fe in the freeze-dried LiS-r was Fe(II) (Table 1), thus indicating minimal reoxidation during the Li^+-saturation, washing, and drying treatments. Some reoxidation occurred during the heat treatment (24 h at 260°C) to invoke Li^+ fix-

https://doi.org/10.1346/CCMN.1999.0470407 Published online by Cambridge University Press

Table 1. Sample labels, treatments, and Fe(II) content (Fe(II)/total Fe). CA = Chemical analysis, MS = Mössbauer spectroscopy.

Sample	NaS	LiS	NaS-r	LiS-r	LiS-rh	LiS-h	LiS-rho
Treatment	—	—	reduction	reduction	reduction heating	— heating	reduction heating reoxidation
Fe(II)/Fe CA	<0.002	<0.002	0.94	0.83	0.71	<0.002	0.21
MS	0	n.d.	0.89	n.d.	n.d.	n.d.	0.23

ation. However, 71% of total Fe was Fe(II) in the heat-treated clay (Table 1). Purging oxygen through the clay mineral suspension reoxidized additional Fe(II), however, after freeze-drying, the reoxidized smectite contained >20% of total Fe as Fe(II) (Table 1). By contrast, the reoxidation treatment causes complete reoxidation of Fe(II) in reduced Na-saturated smectites (Komadel *et al.*, 1990, 1995). Both the chemical and Mössbauer (Figure 1) data offer convincing evidence that Li^+ fixation in highly reduced SWa-1 ferruginous smectite caused partial stabilization of Fe(II) in the clay structure.

FTIR spectroscopy

The FTIR spectrum of sample NaS shows a broad OH-stretching band at 3573 cm^{-1} (Figure 2), which reflects the high content of octahedral Fe in the sample (Goodman *et al.*, 1976). No significant change in the position of the OH-stretching band was observed in the FTIR spectrum of the reduced NaS-r other than a slight broadening of the band in the region near 3620 cm^{-1}. Heating for 24 h at 260°C to invoke Li^+ fixation in the unreduced LiS caused only a minor shift of the OH-stretching band from 3575 to 3579 cm^{-1} in LiS-h (Figure 2), showing a partial decrease of the layer charge due to limited fixation of Li in the hexagonal cavities. A similar increase in the position of the OH-stretching band with decreasing layer charge, and thus with the decreasing charge deficiency on apical oxygens, was observed for micas (Robert and Kodama, 1988). By contrast, the OH-stretching band in the spectrum of the reduced-Li-fixed-reoxidized sample, LiS-rho, is markedly different from the other spectra shown in Figure 2. The OH-stretching band in the spectrum of LiS-rho is shifted to 3622 cm^{-1} with a shoulder near 3650 cm^{-1}.

The position of the OH-stretching band of 2:1 phyllosilicates is strongly influenced by nearest-neighbor cations, because they control both the charge balance on oxygen atoms of OH groups and the orientation of the OH dipole (Farmer, 1974; Robert and Kodama, 1988). Previous IR studies of celadonites and glauconites (Slonimskaya *et al.*, 1986) and smectites (Madejová *et al.*, 1994, 1996) showed that the OH-stretching band could be reliably resolved into the individual

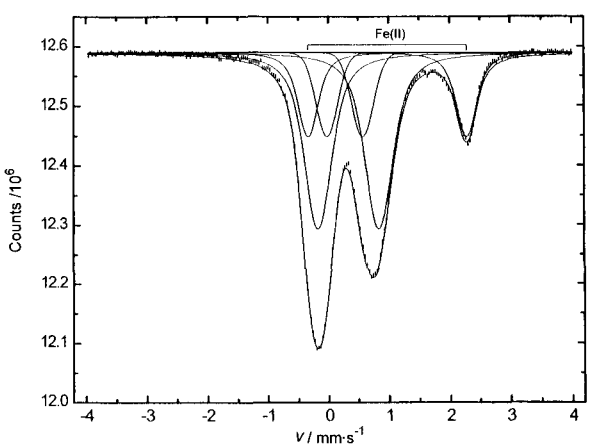

Figure 1. Mössbauer spectrum at 90 K of SWa-1 after reduction, Li^+-fixation, and reoxidation (sample LiS-rho).

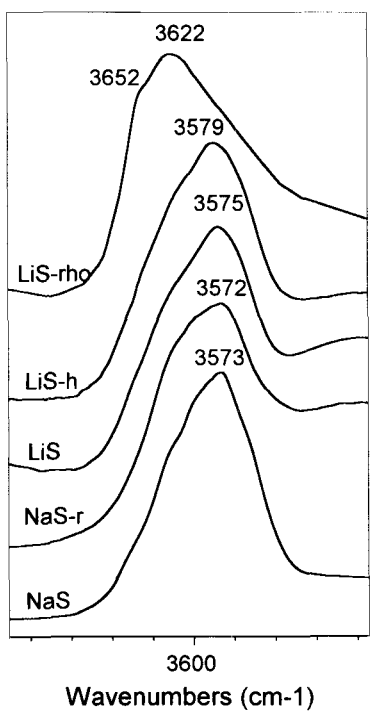

Figure 2. FTIR spectra of SWa-1 samples in OH-stretching region. NaS and NaS-r are Na^+-saturated SWa-1 untreated and reduced, respectively. Sample descriptions and treatments of other samples are listed in Table 1.

https://doi.org/10.1346/CCMN.1999.0470407 Published online by Cambridge University Press

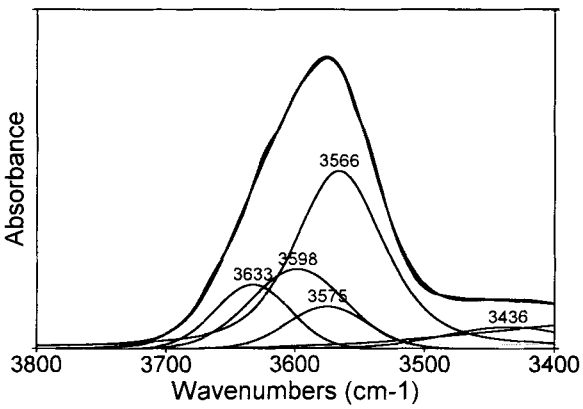

Figure 3. Decomposition of the FTIR spectrum of unaltered SWa-1 (sample LiS); experimental and calculated curves and the OH components (Table 2).

components corresponding to OH coordinated to specific groupings of octahedral atoms. A similar approach was used here to study the changes in the IR spectra of SWa-1.

The OH groups associated with Fe(III)Fe(III) (3566 cm^{-1}), Fe(III)Mg(3575 cm^{-1}), AlFe(III) (3598 cm^{-1}), and AlAl (3633 cm^{-1}) pairs are expected to dominate the unaltered sample (Figure 3; Table 2). The pronounced shift in the OH-stretching band to 3622 cm^{-1} in the spectrum of LiS-rho is due to new OH components absorbing at higher wavenumbers. For dioctahedral smectites, only AlAlOH groups are known to absorb in this region (Farmer, 1974; Madejová *et al.*, 1994, 1996). However, the number of AlAl pairs cannot be substantially higher in LiS-rho than in the LiS sample. Therefore, the new components at 3656 and 3623 cm^{-1}, obtained by decomposition of the OH band in the FTIR spectrum of LiS-rho, are assigned to new groupings developed in the mineral structure upon treatment (Figure 4; Table 2). During heating, Li^+ cations are widely considered to migrate from the interlayer into the vacant octahedra, near sites of isomorphous substitution. Pairs of AlFe(II) and Fe(III)Fe(II) created during Fe(III) reduction attract Li to the vacant octahedra near by. Li fixation creates local trioctahedral configurations of AlFe(II)Li and Fe(III)Fe(II)Li. Calvet and Prost (1971) and Madejová *et al.* (1996) reported the bands near 3670 and 3660 cm^{-1}, respectively, to be due to an AlMgLi configuration. According to Vedder (1964), substitution of Mg by Fe(II) in talc shifts the ν_{OH} downward by ~16 cm^{-1}. The component band observed at 3656 cm^{-1} may, therefore, be related to OH in an AlFe(II)Li configuration. Absorption bands in the 3660–3650 cm^{-1} region assigned to an AlFe(II)Li configuration were found in the spectra of natural Li-Fe-Al-micas (Von Goldstein *et al.*, 1995). The assignment of the component at 3623 cm^{-1} in the spectrum LiS-rho is based on the presumption that the difference in the positions of AlFe(II)LiOH and Fe(III)Fe(II)LiOH components should be very close to that of AlFeOH and FeFeOH components in the spectrum of LiS, *i.e.*, close to 32 cm^{-1} (Table 2). The AlFe(II)LiOH groups absorb at 3656 cm^{-1}, therefore the absorption at 3623 cm^{-1} is believed to be due to Fe(III)Fe(II)LiOH groups.

Table 2. Assignments, positions, and areas of the OH components of the spectra shown in Figures 3 and 4.

	LiS		LiS-rho	
Assignment	$\bar{\nu}$ (cm^{-1})	Area (%)	$\bar{\nu}$ (cm^{-1})	Area (%)
AlFe(II)LiOH	—	—	3656	13.97
AlAlOH	3633	13.42	3637	13.97
Fe(III)Fe(II)LiOH	—	—	3623	22.28
AlFe(III)OH	3598	21.09	3599	11.32
Fe(III)MgOH	3575	9.32	3582	8.31
Fe(III)Fe(III)OH	3566	56.17	3561	30.15

Deconvolution of the OH-stretching bands for LiS and LiS-rho yielded positions, assignments, and areas of individual OH components. The area under an absorption-band curve is proportional to the concentration of the absorbing group and the absorption coefficient. However, Rouxhet (1970) found that within the same type of minerals the absorption coefficient per OH group was about the same and did not depend appreciably on either the chemical composition or the orientation of the oscillator. This assumption was used effectively as a basis for the determination of the octahedral cation content (Slonimskaya *et al.*, 1986; Madejová *et al.*, 1996; Besson and Drits, 1997b). Thus, areas shown in Table 2 are assumed to be proportional to concentrations of OH groups in the variously assigned coordination environments. The decrease in the areas of AlFe(III)OH and Fe(III)Fe(III)OH components of LiS-rho as compared to LiS, reflects that AlFe(III) and Fe(III)Fe(III) pairs in LiS were partially replaced with AlFe(II)Li and Fe(III)Fe(II)Li, respec-

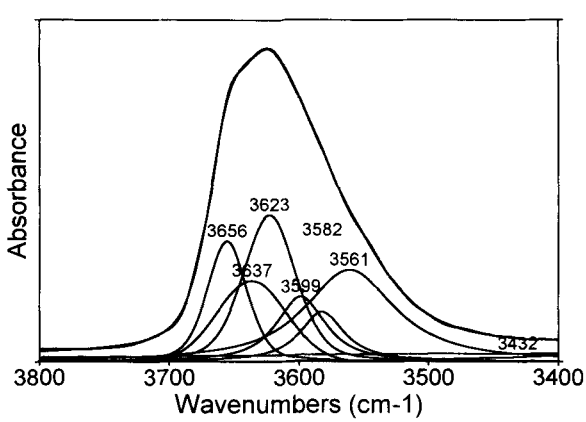

Figure 4. Decomposition of the FTIR spectrum of SWa-1 after the treatments (sample LiS-rho); experimental and calculated curves and the OH components (Table 2).

https://doi.org/10.1346/CCMN.1999.0470407 Published online by Cambridge University Press

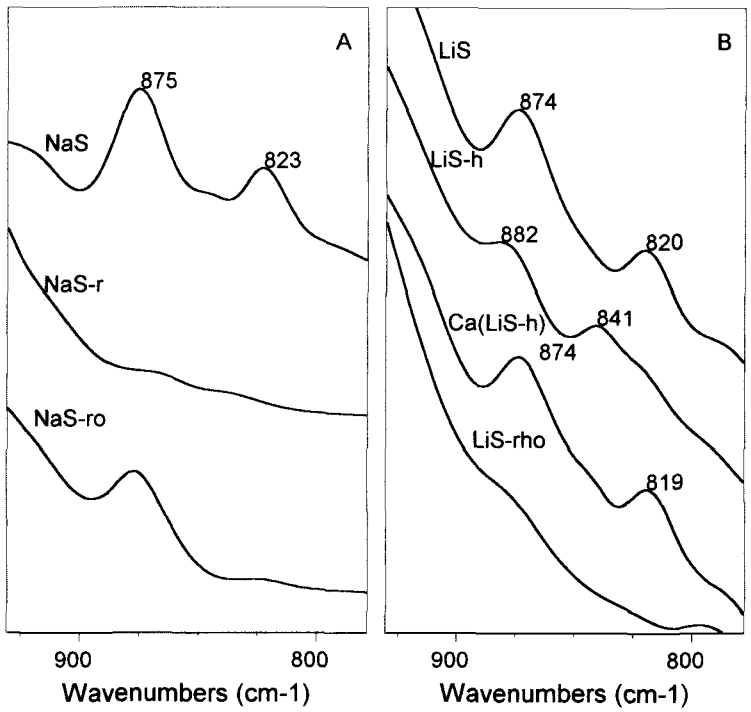

Figure 5. A) FTIR spectra of Na^+-saturated SWa-1 samples in OH-bending region. NaS: untreated, NaS-r: reduced, NaS-ro: reduced and reoxidized. B) FTIR spectra of samples described in Table 1, Ca(LiS-h) is Ca^{2+}-exchanged LiS-h sample.

tively. Similar values of AlAl and Fe(III)Mg areas observed for LiS and LiS-rho samples indicated that migration of Li^+ ions close to this OH group is improbable.

Areas of individual OH components with Fe(II) in their coordination sphere allowed calculation of the Fe(II)/total Fe ratio in LiS-rho. This calculation assumes that the concentration of each cation is equal to the sum of the contributions of the cations to the areas of OH groups, which contain the given cation in their nearest environment (Slonimskaya *et al.*, 1986). The result obtained, 20% of total Fe as Fe(II), is in excellent agreement with both chemical and Mössbauer data (Table 1).

The 950–800 cm^{-1} region provides complementary evidence for Li migration into the structure upon heating. The FTIR spectrum of the NaS sample contains the bands associated with OH-bending vibrations at 875 and 823 cm^{-1} due to AlFeOH and FeFeOH groups, respectively (Figure 5A). After reduction of >80% of the total Fe to Fe(II), the OH-bending bands were almost lost and only very slight inflections are distinguishable in the spectrum of NaS-r. During reduction, the free radicals (SO_2^-) transfer electrons to structural Fe(III), reducing it to Fe(II). The structure of the clay mineral becomes destabilized by an excess negative charge causing partial dehydroxylation, deprotonation, and/or other crystalline rearangements (Komadel *et al.*, 1995; Gates *et al.*, 1996; Sucki *et al.*, 1996). The more acidic character of OH groups coordinated by Fe(III), as a result of the greater electron affinity of Fe(III) compared with Al(III), contributes to preferential deprotonation of FeFeOH groups (Russell, 1979). Reoxidation of the sample partially restored the AlFeOH band in the FTIR spectrum of sample NaS-ro, thus proving the presence of a significant number of AlFeOH groups, where only a weak inflection near 820 cm^{-1} indicates the presence of only a few FeFeOH groups in sample NaS-ro (Figure 5A).

Notable changes were observed in the OH-bending region when unreduced LiS was heated to 260°C to fix Li^+ ions (spectrum LiS-h in Figure 5B). Due to the prevailing tetrahedral charge of this clay mineral, most of the Li^+ was trapped in the hexagonal holes of the tetrahedral sheet. The shift of the AlFeOH band to 882 cm^{-1} and the appearance of an FeFeOH band at 841 cm^{-1} with a shoulder near 820 cm^{-1}, as well as the decrease in intensities of both of these bands (Figure 5B), indicates a significant perturbation of OH-bending vibrations in LiS-h due to Li^+ located directly above or below the structural OH groups. These Li^+ ions affect the direction of the dipole moment of the OH groups and perturb its deformation vibration energy (McBride and Mortland, 1974). After exchangeable Li^+ ions in LiS-h were exchanged by Ca^{2+}, the IR spectrum regained the shape of the untreated sample (see spectra LiS and Ca(LiS-h) in Figure 5B). This ion-exchange treatment allowed the layers to swell and

https://doi.org/10.1346/CCMN.1999.0470407 Published online by Cambridge University Press

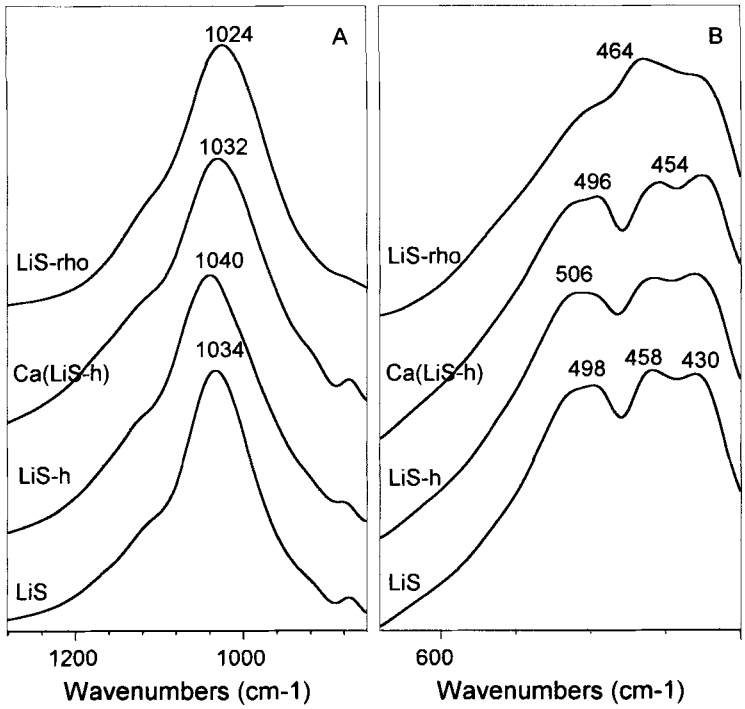

Figure 6. FTIR spectra of LiS, LiS-h, Ca(LiS-h), LiS-rho samples in (A) the Si-O stretching and (B) bending regions. Sample descriptions and treatments of other samples are listed in Table 1.

the Li^+ ions in the hexagonal holes to rehydrate and move from these sites. The similarity of the spectra for LiS and Ca(LiS-h) samples confirms that most Li^+ ions were trapped reversibly in the structure of LiS-h, whereas the number of Li^+ ions possibly fixed irreversibly to compensate for octahedral charge is below the detection limit of IR spectroscopy.

Reduction of Fe(III) in SWa-1 increased the negative charge in the octahedral sheet, but also increased the extent to which Li fixation occurred upon heating, which compensated some of the increased charge. The OH-bending region in the spectrum of sample LiS-rho (Figure 5B) reflects substantial structural changes owing to the treatments. In comparison with the spectra of samples NaS-ro (Figure 5A) and Ca(LiS-h) (Figure 5B), no bands relating to OH vibrations (except only a very weak inflection near 875 cm^{-1} due to AlFe(III)OH) are present in the spectrum of sample LiS-rho. Both reduction and Li fixation contribute to the observed decrease in the band intensities of structural OH groups in the 900–800 cm^{-1} region. Komadel *et al.* (1995) found that structural OH content in reduced-reoxidized nontronite is ~15–20% less than in the original sample, thus proving partial dehydroxylation of reduced-reoxidized mineral. As discussed above, deprotonation can possibly contribute to lower OH content. Li fixation in LiS-r causes partial replacement of OH groups shared by one empty octahedron and two octahedra with trivalent central atoms (which is common for dioctahedral smectites), *i.e.*, AlFe(III)OH and Fe(III)Fe(III)OH groups, with OH groups shared by three octahedra with central atoms (typical for trioctahedral smectites), which absorb in the 700–660 cm^{-1} region. Their bands cannot be distinguished in the spectrum of LiS-rho because they are overlapped by the intensive Fe-O out-of-plane vibration centered at 678 cm^{-1} (Farmer, 1974; Russell and Fraser, 1994). Moreover, the ability of Li^+ ions in hexagonal holes to perturb OH-deformation vibrations and decrease their intensities (spectrum LiS-h in Figure 5B), contributes to the near complete disappearance of OH-bending bands in the spectrum of sample LiS-rho (Figure 5B).

Further changes occurred in the Si-O stretching and bending regions (Figure 6). The Si-O stretching band, observed at 1034 cm^{-1} for LiS, shifted to 1040 cm^{-1} upon heating (see spectrum LiS-h in Figure 6A). A similar shift to higher wavenumbers, found for heated Li-montmorillonite, indicates a decrease of the layer charge due to the presence of Li either in hexagonal holes or in the previously vacant octahedra (Madejová *et al.*, 1996). After Ca^{2+} was exchanged for Li^+ in the LiS-h sample, the Si-O band returned to 1032 cm^{-1} (spectrum of Ca(LiS-h) in Figure 6A). This shift confirmed that Li^+ in the hexagonal holes of the tetrahedral sheet can be exchanged by Ca^{2+}. Thus, this Li^{2+} is not really fixed. However, the shift of the Si-O stretching band to 1024 cm^{-1} in the spectrum of LiS-

https://doi.org/10.1346/CCMN.1999.0470407 Published online by Cambridge University Press

rho (Figure 6A) reflects the effect of Fe(II) in the re-oxidized sample on the Si-O vibrations. A similar downward shift upon reduction was reported in the spectra of reduced nontronites (Stucki and Roth, 1976; Rozenson and Heller-Kallai, 1976; Komadel *et al.*, 1995).

Three absorption bands, Si-O-Fe at 498 and 430 cm^{-1} and Si-O-Si at 458 cm^{-1}, were observed in the Si-O bending region in the spectrum of the LiS sample (Figure 6B). A shoulder near 510 cm^{-1} (related to Al-O-Si bending vibration) indicated the presence of Al in the octahedra. No significant changes were observed for unreduced heated samples (see spectra LiS-h and Ca(LiS-h) in Figure 6B). However, a pronounced decrease in intensity of both Si-O-Fe bands caused coalescence of the bands into a broad, diffuse band at ~464 cm^{-1} in the spectrum of LiS-rho sample. These spectral changes are consistent with significant changes in bonding and/or symmetry of octahedral Fe, including interactions with other octahedral cations and with the tetrahedral sheet. They may arise from the change in Fe oxidation state only (Gates *et al.*, 1996), or they may be the result of more extensive alterations within the structure.

CONCLUSIONS

Partial stabilization of Fe(II) in reduced dioctahedral smectites can be accomplished after Li saturation and after heating the Li form of a highly reduced clay in N_2 atmosphere at 260°C for 24 h to produce Li fixation in the smectite structure. This treatment led to stabilization of >20% of total Fe as Fe(II) in ferruginous smectite SWa-1. Decomposition of the OH-stretching band in the IR spectra proved that part of the Li^+ was trapped in previously vacant octahedral sites. Some of the OH groups in the reoxidized smectite were associated with trioctahedral AlFe(II)Li or Fe(III)Fe(II)Li groupings of central atoms in the octahedral sheets.

ACKNOWLEDGMENTS

The authors thank D. Huo for reducing the Na-SWa-1 sample and providing its FTIR spectrum. They thank also the Slovak-US Science and Technology Program (grant 94055) and the Slovak Grant Agency VEGA (grant 2/4042/98), which provided partial financial support for this study.

REFERENCES

Alvero, R., Alba, M.D., Castro, M.A., and Trillo, J.M. (1994) Reversible migration of lithium in montmorillonite. *Journal of Physical Chemistry*, **98,** 7848–7853.

Besson, G. and Drits, V.A. (1997a) Refined relationships between chemical composition of dioctahedral fine-grained mica minerals and their infrared spectra within the OH stretching region. Part I: Identification of the OH stretching bands. *Clays and Clay Minerals*, **45,** 158–169.

Besson, G. and Drits, V.A. (1997b) Refined relationships between chemical composition of dioctahedral fine-grained mica minerals and their infrared spectra within the OH stretching region. Part II: The main factors affecting OH vibrations and quantitative analysis. *Clays and Clay Minerals*, **45,** 170–183.

Breen, C., Zahoor, F.D., Madejová, J., and Komadel, P. (1997) Characterisation and catalytic activity of acid treated, size fractionated smectites. *Journal of Physical Chemistry B*, **101,** 5324–5331.

Bujdák, J. and Slosiariková, H. (1994) Dehydration and dehydroxylation of reduced-charge montmorillonite. *Journal of Thermal Analysis*, **41,** 825–831.

Bujdák, J., Slosiariková, H., Nováková, L'., and Číčel, B. (1991) Fixation of lithium cations in montmorillonite. *Chemical Papers*, **45,** 499–507.

Bujdák, J., Petrovičová, I., and Slosiariková, H. (1992a) Study of water-reduced charge montmorillonite system. *Geologica Carpathica Series Clays*, **43,** 109–111.

Bujdák, J., Slosiariková, H., and Číčel, B. (1992b) Interaction of long chain alkylammonium cations with reduced charge montmorillonite. *Journal of Inclusion Phenomena and Molecular Recognition*, **13,** 321–327.

Bujdák, J., Slosiariková, H., and Číčel, B. (1993) Sorption of hexadecylammonium ions on reduced charge montmorillonite. *Chemical Papers*, **47,** 85–87.

Calvet, R. and Prost, R. (1971) Cation migration into empty octahedral sites and surface properties of clays. *Clays and Clay Minerals*, **19,** 175–186.

Gates, W.P., Stucki, J.W., and Kirkpatrick, R.J. (1996) Structural properties of reduced Upton montmorillonite. *Physics and Chemistry of Minerals*, **23,** 535–541.

Goodman, B.A., Russell, J.D., and Fraser, A.R. (1976) A Mössbauer and IR spectroscopic study of the structure of nontronite. *Clays and Clay Minerals*, **24,** 53–59.

Greene-Kelly R. (1953) The identification of montmorillonoids in clays. *Journal of Soil Science*, **4,** 233–237.

Farmer, V.C. (1974) Layer silicates. In *Infrared Spectra of Minerals*, V.C. Farmer, ed., Mineralogical Society, London, 331–363.

Hofmann, U. and Klemen, R. (1950) Verlust der Austauschfähigkeit von Lithiuminonen an Bentonit durch Erhitzung. *Zeitschrift für Anorganische und Allgemeine Chemie*, **262,** 95–99.

Komadel, P. and Stucki, J.W. (1988) The quantitative assay of minerals for Fe^{2+} and Fe^{3+} using 1,10-phenanthroline: A rapid photochemical method. *Clays and Clay Minerals*, **36,** 379–381.

Komadel, P., Lear, P.R., and Stucki, J.W. (1990) Reduction and reoxidation of nontronite: Extent of reduction and reaction rates. *Clays and Clay Minerals*, **38,** 203–208.

Komadel, P., Madejová, J., and Stucki, J.W. (1995) Reduction and reoxidation of nontronite: Questions of reversibility. *Clays and Clay Minerals*, **43,** 105–110.

Komadel, P., Bujdák, J., Madejová, J., Šucha, V., and Elsass, F. (1996a) Effect of non-swelling layers on the dissolution of reduced-charge montmorillonite in hydrochloric acid. *Clay Minerals*, **31,** 333–345.

Komadel, P., Madejová, J., Janek, M., Gates, W.P., Kirkpatrick, R.J., and Stucki, J.W. (1996b) Dissolution of hectorite in inorganic acids. *Clays and Clay Minerals*, **44,** 228–236.

Lim, C.H. and Jackson, M.L. (1986) Expandable phyllosilicate reactions with lithium on heating. *Clays and Clay Minerals*, **34,** 346–352.

Madejová, J., Komadel, P., and Číčel, B. (1994) Infrared study of octahedral site populations in smectites. *Clay Minerals*, **31,** 319–326.

Madejová, J., Bujdák, J., Gates, W.P., and Komadel, P. (1996) Preparation and infrared spectroscopic characterization of reduced-charge montmorillonite with various Li content. *Clay Minerals*, **31,** 233–241.

Manceau, A., Drits, V.A., Lanson, B., Chateigner, D., Wu, J., Huo, D., Gates, W.P., and Stucki, J.W. (1999) Oxidation-reduction mechanism of iron in dioctahedral smectites. 2. Structural chemistry of reduced Garfield nontronite. *American Mineralogist*, in press.

McBride, M.B., and Mortland, M.M. (1974) Copper (II) interactions with montmorillonite: Evidence from physical methods. *Soil Science Society of America Proceedings*, **38,** 408–415.

Robert, J.L. and Kodama, H. (1988) Generalization of the correlations between hydroxyl-stretching wavenumbers and composition of micas in the system K_2O-MgO-Al_2O_3-SiO_2-H_2O: A single model for trioctahedral and dioctahedral micas. *American Journal of Science*, **228A,** 196–212.

Rouxhet, P.G. (1970) Hydroxyl stretching bands in micas: A quantitative interpretation. *Clay Minerals*, **8,** 375–388.

Rozenson, I. and Heller-Kallai, L. (1976) Reduction and oxidation of Fe^{3+} in dioctahedral smectite. I.: Reduction with hydrazine and dithionite. *Clays and Clay Minerals*, **32,** 271–282.

Russell, J.D. (1979) An infrared spectroscopic study of interaction of nontronite and ferruginous montmorillonites with alkali metal hydroxides. *Clay Minerals*, **14,** 127–137.

Russell, J.D. and Fraser, A.R. (1994) Infrared methods. In *Clay Mineralogy: Spectroscopic and Chemical Determinative Methods*, M.J. Wilson, ed., Chapman & Hall, London, 11–67.

Shen, S. and Stucki, J.W. (1994) Effects of iron oxidation state on the fate and behavior of potassium in soils. In *Soil Testing: Prospects for Improving Nutrient Recommendations*, J.L. Havlin, J. Jacobsen, P. Fixen, and G. Hergert, eds., Soil Science Society of America Special Publication 40, Soil Science Society of America, Madison, Wisconsin, 173–185.

Shen, S., Stucki, J.W., and Boast C.W. (1992). Effects of structural iron reduction on the hydraulic conductivity of Na-smectite. *Clays and Clay Minerals*, **40,** 381–386.

Slonimskaya, M.V., Besson, G., Danyak, L.G., Tchoubar, C., and Drits, V.A. (1986) Interpretation of the IR spectra of celadonites and glauconites in the region of OH-stretching frequencies. *Clay Minerals*, **21,** 115–149.

Stucki, J.W. (1988) Structural iron in smectites. In *Iron in Soils and Clay Minerals*, J.W. Stucki, B.A. Goodman, and U. Schwertmann, eds., D. Reidel, Dordrecht, 625–675.

Stucki, J.W. and Roth, C.B. (1976) Interpretation of infrared spectra of oxidized and reduced nontronite. *Clays and Clay Minerals*, **24,** 293–296.

Stucki, J.W., Golden, D.C., and Roth, C.B. (1984) The preparation and handling of dithionite-reduced smectite suspensions. *Clays and Clay Minerals*, **32,** 191–197.

Stucki, J.W., Bailey, G.W., and Gan, H. (1996) Oxidation-reduction mechanisms in iron-bearing phyllosilicates. *Applied Clay Science*, **10,** 417–430.

Theng, B.K.G., Hayashi, S., Soma, M., and Seyama, H. (1997) Nuclear magnetic resonance and X-ray photoelectron spectroscopic investigation of lithium migration in montmorillonite. *Clays and Clay Minerals*, **45,** 718–723.

Vedder, W. (1964) Correlations between infrared spectrum and chemical composition of mica. *American Mineralogist*, **49,** 736–768.

Von Goldstein, S., Wolf, D., and Uhlig, J. (1995) Infrared spectroscopic studies on natural Li-Fe-Al micas. *Chemie der Erde*, **55,** 46–60.

(Received 11 June 1998; accepted 17 December 1998; Ms. 98-073)